Enabling Steady Graphite Anode Cycling with High Voltage, Additive-Free, Sulfolane-Based Electrolyte: Role of the Binder

Tong Zhang[1], Iratxe de Meatza[2], Xin Qi[3], Elie Paillard[1]*

[1]*Helmholtz Institute Münster – Forschungszentrum Jülich (IEK-12), Corrensstr. 46, 48149 Münster, Germany*

[2]*IK4-CIDETEC, Parque Tecnológico de San Sebastián, Paseo Miramon 196, 20014 Donostia-San Sebastian, Spain*

[3]*MEET Battery Research Center, University of Muenster, Corrensstr. 46, 48149 Münster, Germany*

Abstract

We demonstrate here the possibility of operating both high voltage spinel and high mass loading graphite electrodes in a 1M $LiPF_6$ in SL/DMC (1/1, wt/wt) electrolyte without the use of additive. A crucial point for practical graphite electrode operation is the use of the cheaper and environmentally friendly carboxymethyl cellulose (CMC)/styrene-butadiene rubber (SBR) combination instead of the PVDF-based electrodes used in most laboratory studies. With this type of anode we also show the operation of a full Li-ion cell operating at 4.5 V without any additive and show that most of the Li^+ transport limitation observed in half-cells are in fact due to the Li metal counter electrode. The anode binder influence is to be considered for the development of high voltage electrolytes lacking good intrinsic SEI building properties, as the anode binder does not affect cathode performance, contrary to most additives. It opens the route for further improvement by use of SEI forming additives (molecular and salts), keeping in mind the requirement for the cathode.

Keywords: Sulfolane, tetramethylene sulfone, graphite, SEI, carboxymethylcellulose, CMC, PVDF, high voltage spinel, lithium-ion, high voltage electrolyte, additive.

* Corresponding author: e.paillard@fz-juelich.de

1. Introduction

In order to push further the energy density of Li-ion batteries, high voltage cathodes operating above 4.5 V such as $LiNi_{0.5}Mn_{1.5}O_4$ [1] or $LiCoPO_4$ [2] have been proposed since the late 90's. However, these materials are still not implemented in commercial Li-ion batteries, due to the lack of electrolyte able to operate both a graphite anode, necessary for high energy density batteries, and a high voltage cathode. This is linked to the need to build an efficient solid electrolyte interphase (SEI) [3,4] at the surface of graphite for allowing its operation, which has been first achieved by using ethylene carbonate (EC).[5]

In fact, additives such as vinylene carbonate (VC) or fluoroethylene carbonate FEC [6,7] or Li salts, such as lithium bis(oxalate)borate, LiBOB [8], lithium difluoro(oxalate)borate LiDFOB [9] or lithium bis(fluorosulfonyl)imide LiFSI [10,11] can participate in the SEI formation and, in principle, overcome the use of EC. However, it is still a staple for most electrolytes, due to its excellent SEI forming ability and most Li-ion batteries thus use additives combined with EC. Unfortunately, EC is seen as the main weakness for anodic stability and multiple attempts to replace it have been made, in view of operating high voltage cathodes, be it by fluorinated molecules [12,13], dinitriles [14] or sulfones [15,16]

Among its potential substitutes, tetramethylene sulfone (sulfolane, SL, see developed formula in figure 1), was first reported in 1971 in a *'high EMF'* graphite anode cell [17] and later in the 80's for Li metal cells, either as self-standing solvent or in mixtures with ether solvents [18,19], hinting for reasonable SEI formation at low potential. Since then, it has been used, alone or mixed with linear carbonates, for operating high voltage cathodes [2,20]. Furthermore, theoretical studies have recently explained why sulfolane (and alkyl-sulfone in general)-based electrolytes are more stable in oxidation than carbonate-based electrolytes and why this stability would extend to its mixtures with low dielectric solvents such as linear carbonates [21–23], making these electrolytes viable candidates for high voltage Li-ion batteries.

However, only few studies can be found dealing with graphite electrode operation in SL-based electrolytes, and most report only on limited cycling [24-30]. In fact, it is often used in combination with SEI forming agents, such as additives, co-solvents or Li salts and, to the best of our knowledge, no study ever showed practical performance of a graphite electrode in a sulfolane-based electrolyte (namely: high efficiency combined with cycling stability) able, at the same time, to operate up to 4.8 V. This is most likely due to the presence of unsuitable additives or Li salts. In fact, in some cases, graphite and $LiFePO_4$ are operated in SL-based electrolytes [24,25,27], while electrolytes without additives (or SEI forming salts) seem to allow the operation of $Li_5Ti_7O_{12}$ and high voltage cathodes [20]. Among the studied electrolytes, Dahn and coll. reported VC containing SL/ethyl methyl carbonate (EMC) electrolytes able to operate NMC cathodes at 4.5V in full Li-ion cells [28,29], but it should be emphasized that VC has a

anodic stability around 4.6 V itself and that its use above this potential is questionable [31]. Some sulfonyl isocyanate added in 1M LiDFOB solution of SL also allowed for decent graphite cycling, but again, cathode operation was only limited to NMC up to 4.5 V [26].

Thus, we report here on a 1M $LiPF_6$ SL/DMC (1/1, wt/wt) electrolyte and the operation of both a high voltage spinel and graphite electrode in the same electrolyte without the use of any additive. Instead, we compare the influence of the graphite electrode processing in allowing stable cycling of the electrolyte. Indeed, most commercial anodes are water processed using carboxymethyl cellulose (CMC) and styrene-butadiene rubber (SBR) latex as binders, which is a cheaper and environmentally friendly alternative to N-methyl-2-pyrrolidone (NMP) processed PVDF-electrodes. However, most studies only use PVDF laboratory-made electrodes. Thus, we compare here the performance of thin PVDF-based electrodes to a more realistic, high mass loading, CMC-SBR electrode and verify the compatibility of the electrolyte in a full Li-ion operated at 4.5 V as well.

2. Experimental

Electrolyte preparation: SL (Aldrich, 99%) was distilled under vacuum and dried on molecular sieve at 50°C until its water content decreased below 20 ppm as determined by coulometric Karl-Fischer titration (KF 851 Titrando, Mettler Toledo). Dimethyl carbonate (DMC) and $LiPF_6$ (BASF, Selectilyte™) were used as received. The electrolyte was prepared and stored in a Mbraun glove box under argon with O_2 and H_2O content below 0.5 ppm.

Electrode preparation: The $LiNi_{0.43}Mn_{1.5}Cr_{0.07}O_4$ electrodes were prepared by casting a NMP slurry with a solid weight ratio of 85/10/5 ($LiNi_{0.43}Mn_{1.5}Cr_{0.07}O_4$ (Primet Precision Material)/SuperP (Cabot)/PVDF (Solef 5130, SOLVAY)). Active material (AM) mass loading: c.a. 2.6 mg cm^{-2}. The CMC/SBR graphite electrodes were casted using an aqueous slurry with a solid weight ratio of 95/1/2/2 (Graphite (SLX30, Imerys)/SuperC45 (Imerys)/CMC (DOW Wolff CRT30000PA)/SBR (TRD102A, JSR micro)). The CMC has a degree of substitution of c.a. 0.85 and a viscosity at 1% in H_2O between 3000 and 4000 mPa s. AM mass loading: c.a. 6.0 mg cm^{-2}, Thickness: c.a. 70 µm. The PVDF-based graphite electrodes were casted using a NMP slurry, with a 93/2/5 mass ratio (graphite (MAGE, Hitachi chemicals) /SuperC45 (Imerys)/PVDF (5130, Solvay)). AM mass loading: c.a. 3.2 mg cm^{-2}. Thickness: c.a. 53 µm. $LiNi_{0.33}Mn_{0.33}Co_{0.33}O_2$ electrodes were bought from Custom Cells, with mass loading c.a. 14.5 mg cm^{-2} and 86% of active material.

Electrochemical testing: Voltamperometries were done on a VMP potentiostat (BioLogic) in three electrode Swagelok™ cells with Li counter and reference electrodes (Rockwood lithium) at room temperature (c.a. 21-23 °C). Cycling was done on a Maccor 4300 battery cycler in three electrode Swagelok™ cells placed in a temperature-controlled chamber at 20 °C. Conductivity was measured

using a BioLogic MCS10, impedance-based conductimeter, from 60 °C to -40 °C with 30 minutes stabilization every 5 °C.

3. Results and discussion

3.1. Physico-chemical properties of the electrolyte

Figure 1 shows the electrochemical properties of the electrolyte. With a conductivity of 6.1 mS cm^{-1} at 20 °C, the conductivity is in the same range as commercial Li-ion electrolytes such as LP47 (1M $LiPF_6$ EC/DEC 3/7, σ (20 °C) = 4.6 mS cm^{-1}). It is lower than that of LP30 (1M $LiPF_6$, EC/DMC 1/1, σ (20 °C) = 10.1 mS cm^{-1}) as an effect of the higher viscosity and lower dielectric constant of SL as compared to EC. In addition, no crystallization was observed down to -20 °C. While the phase behavior is somehow complicated, given the ternary mixture considered, with 3 different phases forming when going down to -140 °C, the electrolyte, in these conditions, starts crystallizing between -20 °C and -25 °C and fully melts below 0 °C, as seen with the hysteresis between cooling and heating curves. The electrochemical stability window of the electrolyte, shown in the insert together with that of LP30, extends from Li deposition to *c.a.* 5.5 V. The closer zooms reveal small reduction peaks representing *c.a.* 5 µA cm^{-2}, which are commonly seen with Li-ion electrolytes and correspond to surface reactions (including the conversion reaction involving the NiO layer at c.a. 1.5 V [32]) and are, in this case, lower than those of LP30. During the anodic scan, the curves of LP30 and SL-based electrolyte cross several times between 4.5 V and 6 V, the current difference being mostly within experimental error. It is however noticeable that the anodic current with the SL-based electrolyte is lower up to c.a. 4.95 V (and the current density lower than 50 µA cm^{-2}).

The electrochemical stability window seems appropriate for the application, although efficient cycling of graphite depends more on the ability to form a SEI on its surface rather than on an extended stability window.

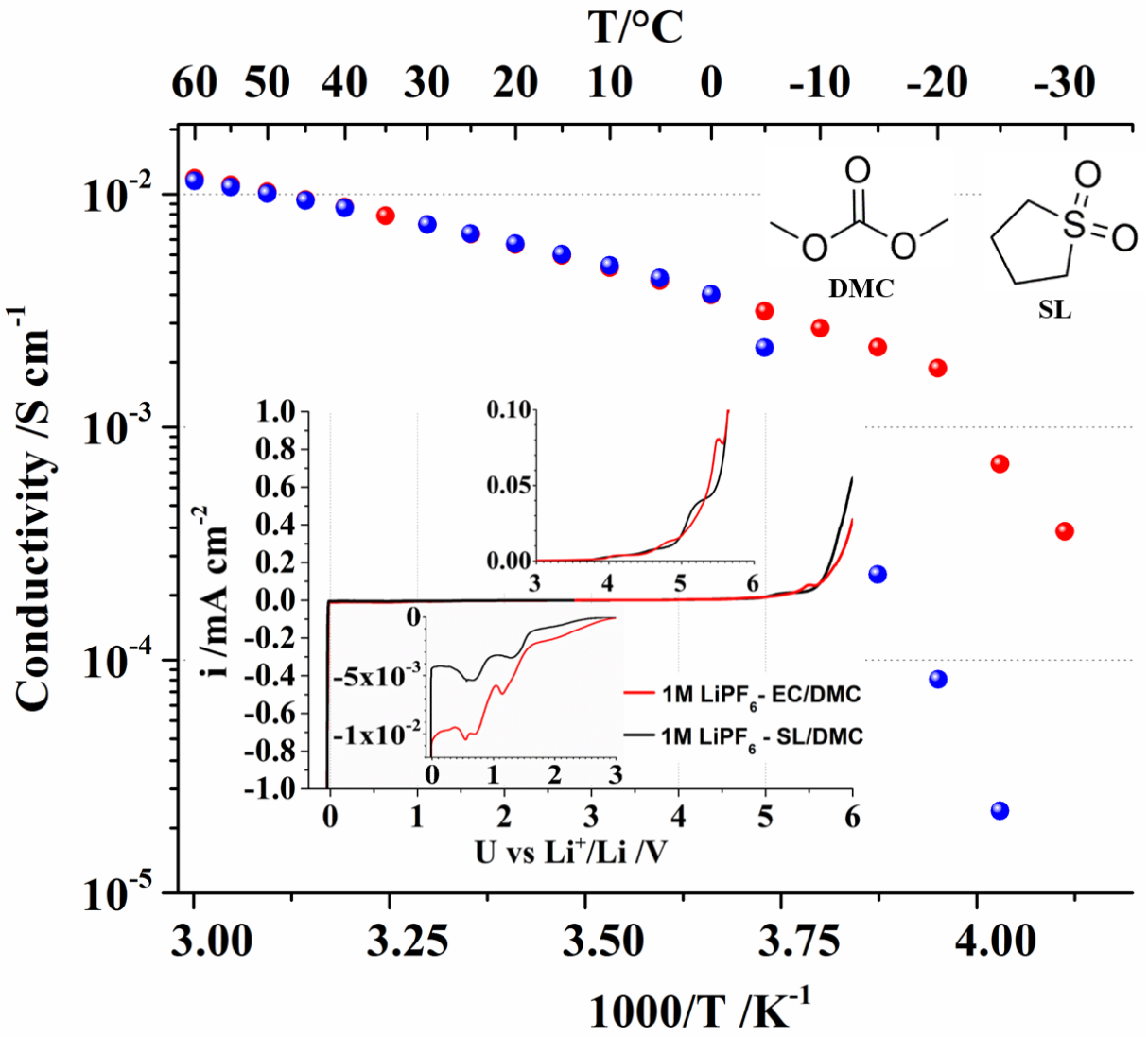

Figure 1: *Arrhenius conductivity plot of the 1M $LiPF_6$ SL/DMC 1/1 (wt/wt) electrolyte.* ***(Insert):*** *Voltamperogram at 0.1 mV s^{-1} on Ni (cathodic scan) and Pt (anodic scan) of 1M $LiPF_6$ in SL/DMC 1/1 (wt/wt) and EC/DMC 1/1 (wt/wt). RE and CE: Li.*

3.2. High voltage spinel

Figure 2 shows the cycling performance of a $LiNi_{0.43}Mn_{1.5}Cr_{0.07}O_4$ electrode. The cycling is steady with 95.1% capacity retention within 90 cycles, which is rather high for the material, especially considering the rather low current density used (C/2) that results in extended contact of the electrolyte with the charged electrode [33]. The capacity fading is probably linked to the Mn dissolution as well as to the limited increase of ohmic drop occurring during cycling, as these are known phenomena for high voltage spinel [34].

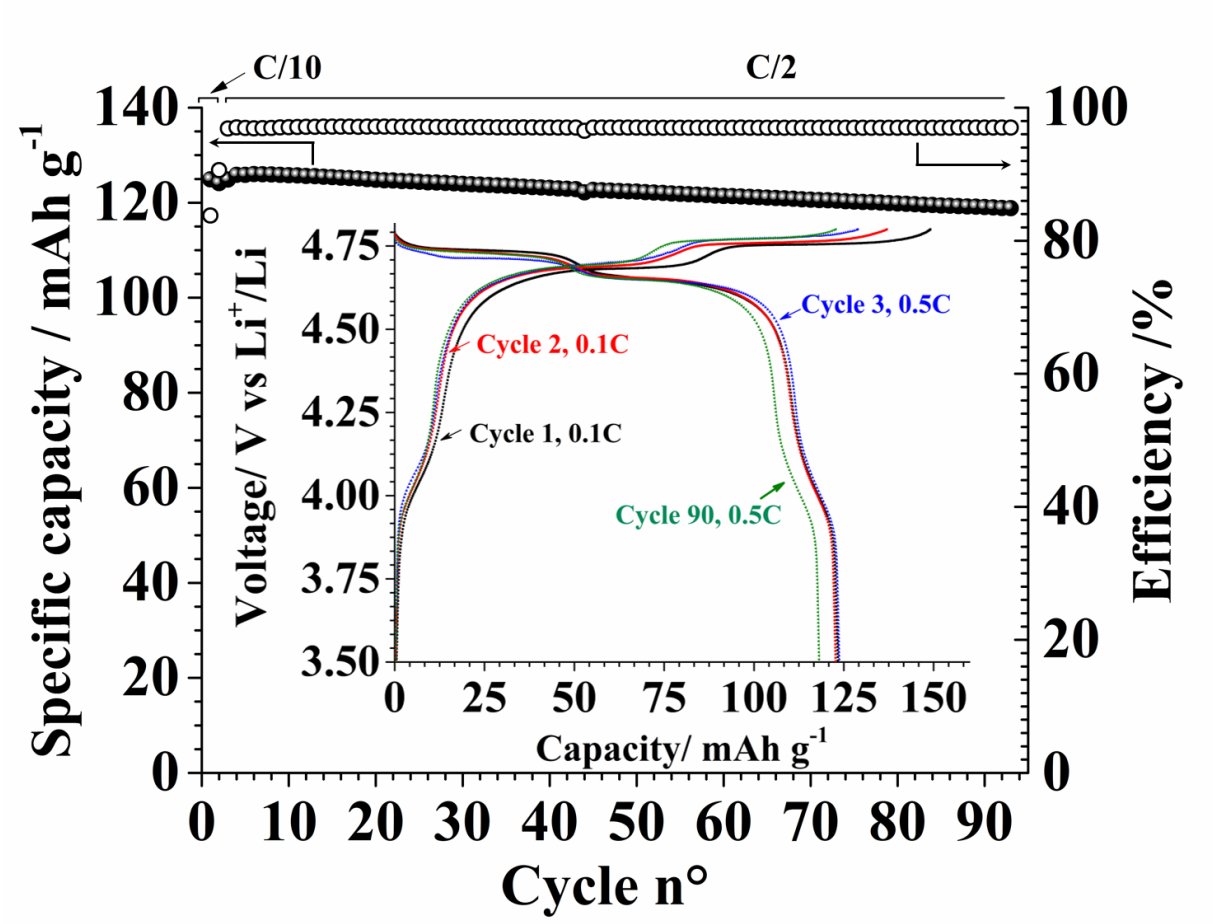

Figure 2. *Discharge capacity and coulombic efficiency of a $LiNi_{0.43}Mn_{1.5}Cr_{0.07}O_4$ electrode in 1M $LiPF_6$ SL/DMC 1/1 (wt/wt) electrolyte.* ***(Insert)****: Voltage profiles for the 1st. 2nd, 3rd and 90th cycles. 1C=147 mA g^{-1}.*

The coulombic efficiency stabilizes above 97% at C/2 with a first cycle efficiency of 83.8% at C/10. It is worth mentioning that decreasing the amount of conductive carbon below 10% (or cycling at higher rate) would likely improve the efficiency.

3.3. Graphite electrodes operation

Figure 3 a. compares the cycling performance of a 3.2 mg cm^{-2} PVDF-based and a 5.4 mg cm^{-2} CMC/SBR-based graphite electrode. For the former, the delivered capacity at C/10 in the first cycle reaches c.a. 320 mAh g^{-1}, but it rapidly decays from the second cycle and does not reach more than 200 mAh g^{-1} at C/2. The first cycle efficiency is below 76%, indicating a strong electrolyte reactivity and, *a priori*, Li consumption for building the SEI. The efficiency then raises as the cycled capacity decreases to around 140 mAh g^{-1} in 60 cycles. The voltage profiles, shown in figure 3.b, reveal a rather high ohmic drop, especially at C/2 and hindered Li^+ transport, probably linked to a resistive SEI. From the second cycle at C/10 most of the Li^+ insertion occurs during the CV step with less than 25 mAh g^{-1} reached at C/2 during Li insertion.

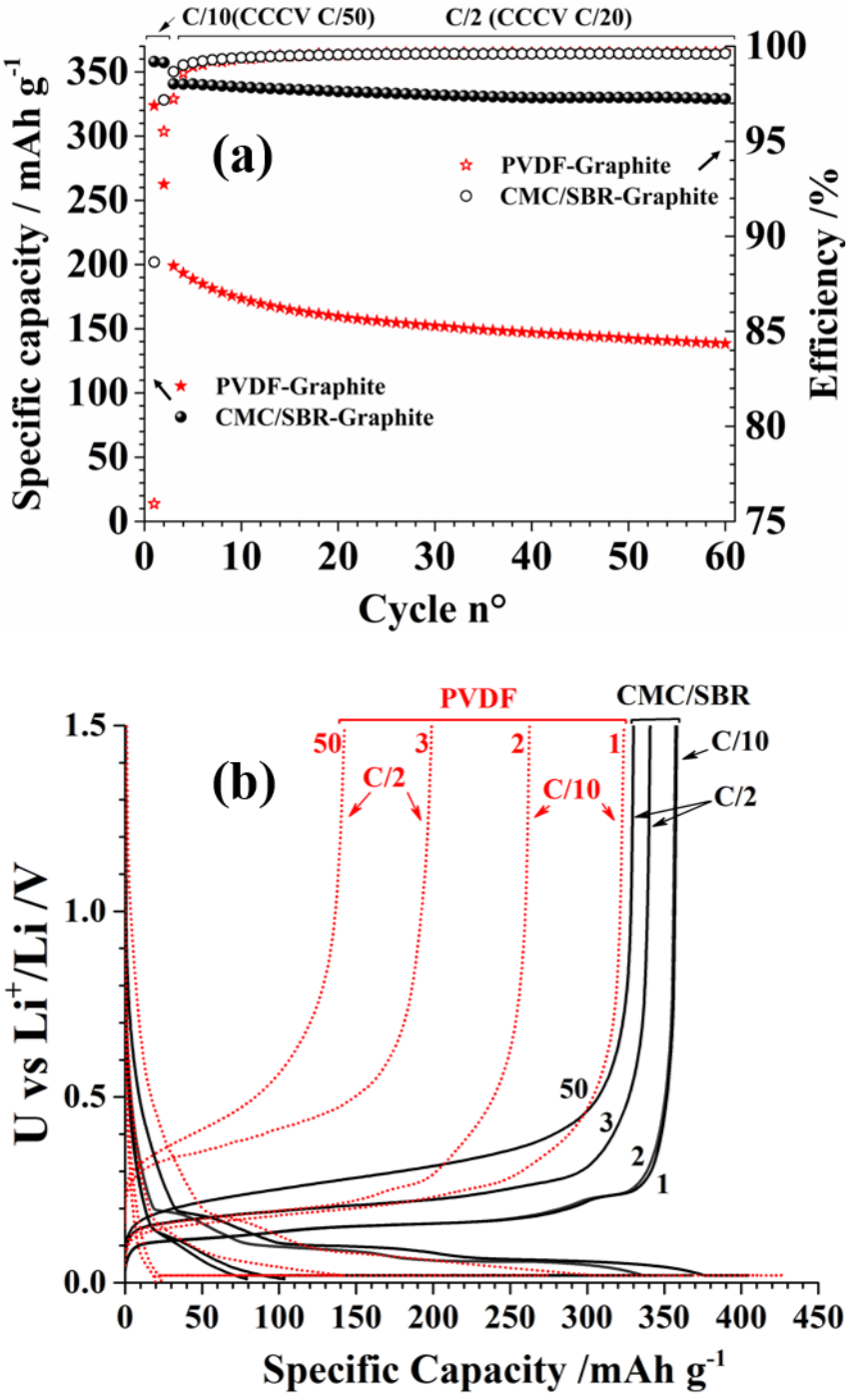

Figure 3. (a) *Comparison of discharge capacity and efficiency between a PVDF-based (3.2 mg cm^{-2} AM mass loading) and a CMC/SBR-based electrode (5.4 mg cm^{-2} AM mass loading)* ***(b)*** *Comparison of the voltage profiles for selected cycles. Cycle numbers are indicated next to the curves. 1C = 372 mA g^{-1}.*

This indicates that the electrolyte forms an SEI, thereby preventing graphite exfoliation and allowing its cycling, but that its formation consumes a large capacity and leads to poor electrode performance, due to a highly resistive SEI which further evolves during cycling. It is coherent with previous studies on graphite cycling in SL-based electrolytes and the use additives such as VC or SEI forming Li salts such as LiBOB, which can help in building a better SEI (i.e. formed with minimal irreversible capacity, stable

with time and cycling, highly electronically resistive, conductive for Li^+ and preventing other electrolyte species to access the graphite surface and react).

On the other hand, the cycling performance of the CMC-SBR-based graphite electrode, displayed in the same figure is far better. An 88.6% coulombic efficiency is reached in the first cycle, which then rises quickly. The capacity at C/10 is *c.a.* 360 mA g^{-1} at C/10 and 340 mA g^{-1} at C/2. The ohmic drop at the beginning of delithiation is still significant, and diffusion limitation increases significantly from cycle 3 to cycle 50 as witnessed by a more marked slope during delithiation. However, the ohmic drop at the beginning of delithiation is strongly reduced (58 mV vs 157 mV in the 3rd cycle at C/2) and Li^+ transport seems much improved as well, despite the mass loading, almost twice.

However, as the SEI on the Li counter electrode can affect ohmic drop and Li^+ transport, and impact the results, full-Li-ion cells were built as well, using commercial NMC electrodes.

3.4. Full cell Graphite/NMC

To suppress the influence of the lithium counter electrode, full Li-ion cells with closely balanced electrodes were assembled. Figure 4 shows the cycling results obtained with a NMC electrode of 2.4 mAh cm^{-2} (at 170 mAh g^{-1}) paired with CMC-SBR graphite electrode of c.a. 2.2 mAh cm^{-2} (at 372 mAh g^{-1}) and cycled between within 2.8 V and 4.5 V. As can be seen, the cycling efficiency is high and reaches 99.7% in these conditions, even with the NMC cut-off potential drifting toward 4.6 V as cycling progresses. Most importantly, the graphite electrode voltage profiles at C/2 (figure 4b) does not show excessive ohmic drop and reduced Li^+ mobility anymore compared to half-cells. Overall, the cell performance is rather good, with charges below 3 h at C/2, including the CV step.

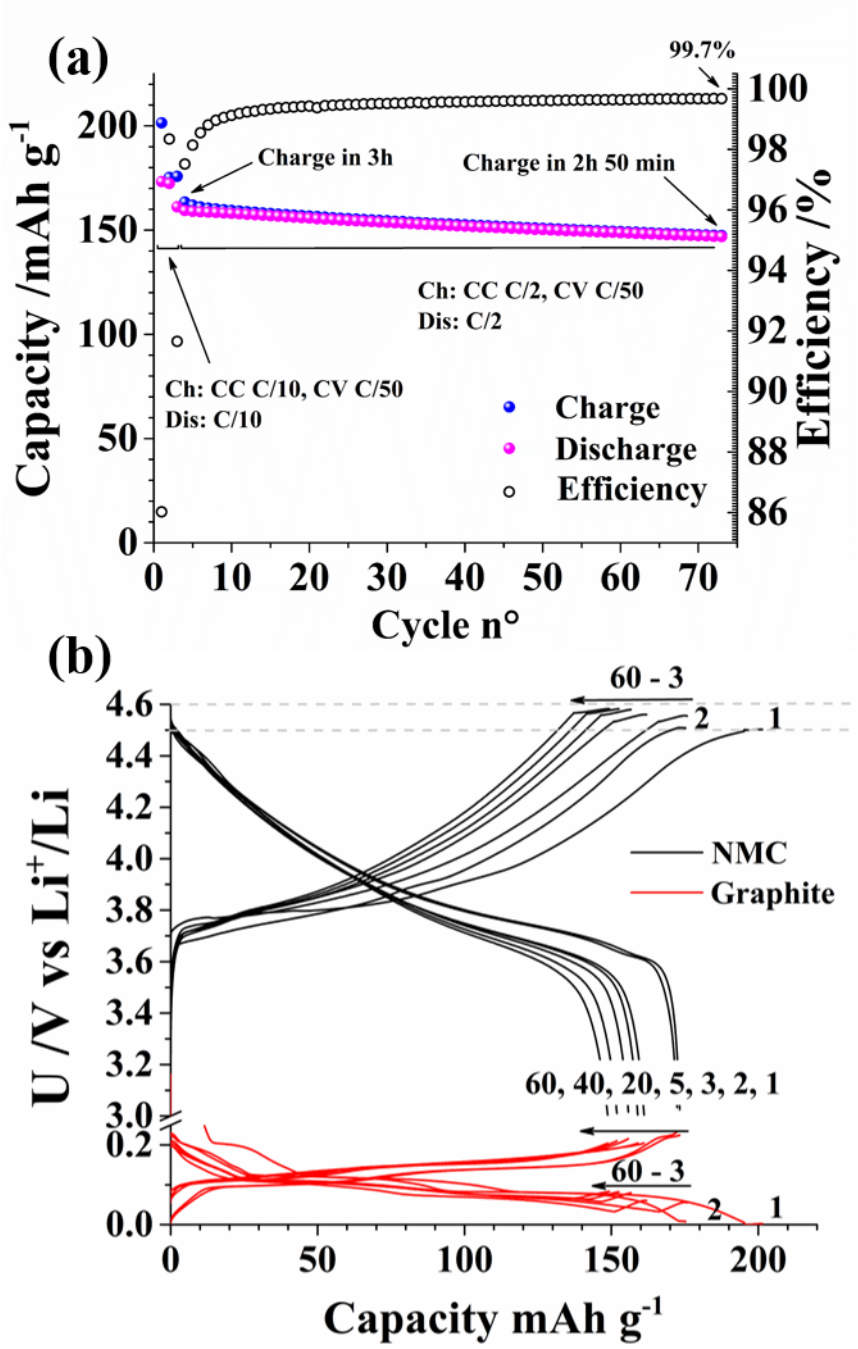

Figure 4. (a) *Capacity retention and cycling efficiency of a Graphite/NMC Li-ion cell (3 electrodes cell, reference electrode: Li metal). AM mass loading cathode: 14.5 mg cm^{-2}, AM mass loading anode: 6 mg cm^{-2}. Voltage range: 2.8 V-4.5 V. Rates indicated on the figure.* ***(b)*** *Corresponding potential profile for the NMC cathode and the graphite anode. Cycle numbers are indicated on the curves.*

It is worth mentioning that Dahn's group has been working in full graphite/NMC cells with industry-made graphite electrodes including both CMC and SBR [28,29], and reported poor cycling of graphite without the use of additives, with a marked reduction peak in dQ/dV curves without VC. However, the CMC content in the electrode was only 1.1% [35] (vs 2% in the present study) which might explain the difference between results (besides the use of EMC instead of DMC). Several grades of CMC are

available on the market, with varying degree of substitution and various chain length, which can also play a role in electrode performance. It is likely that carbon surface groups influence efficient building of the SEI on graphite with SL-based electrolytes as well. It is however clear that CMC helps in building a better SEI. Indeed, it is known from earlier reports on anodes (including carbon) which are challenging for SEI building such as conversion [36], alloying [37-40] or conversion/alloying materials [41], that CMC plays a paramount role in efficient SEI building. Moreover, even if only little differences are observed in carbonate-based electrolytes, its implication in SEI on graphite was also reported [42,43]. The participation of CMC in the SEI building is linked to the fact that CMC contains hydroxyl and carboxylate functional groups and thus tend to coat the particles as thin layer due to the interaction with carbon surface groups, leading to stronger adhesion strength as compared with PVDF [44,45]. It was, in fact, proposed that for polyacrylic acid (PAA), which also contains carboxylate groups, esterification reaction with graphite surface group occur during electrode drying resulting in strong binding by covalent bonds [46]. It then reacts with the electrolytes containing $LiPF_6$ (as it is the case here) by contact and upon reduction to form component that are then found in the SEI [42], whereas PVDF has limited influence on SEI formation.

Although CMC is cheap and its use is widespread as Li-ion electrode binder, other water processable binders such as alginates [47], or PAA [48] are also good candidates which are likely to help in SEI building on graphite with electrolytes having suboptimal SEI forming properties. Finally, although the electrolyte used here does not include any additive, graphite performance would certainly benefit from additive use, such as VC, if the cathodes to be used do not operate above 4.6 V, or from other lithium salts, which should allow improved graphite performance.

4. Conclusion

We show here that the 1M $LiPF_6$ SL/DMC (1/1, wt/wt) electrolyte is able to operate both high voltage spinel and a CMC/SBR-based graphite anode without the use of any additive, thanks to the use of CMC as binder. As the SL-based electrolyte is not ideal for half-cells studies, due to poor Li^+ transport at the electrolyte/Li metal interface, full Li-ion cell operating at 4.5 V without additive were also assembled, resulting in good graphite electrode (and overall) performance. This will surely pave the way for further electrolyte development as many additives are available for increasing further the SEI quality on these types of anode. It is especially worth emphasizing that SEI building is a multi-parameter process in which electrode materials, electrolyte, as well as processing of the electrodes all play a role. It is likely that optimized SL-based electrolytes will lead to higher performance that the one described here, based on $LiPF_6$, which is neither the most conductive salt, nor the best performing salt vs graphite. However, the choice of Li salt and additive depends on the target anodic stability, be it 4.6 V or 4.8 V, whereas the anode binder, in principle, does not affect cathode performance.

Acknowledgements

The research leading to these results is part of the 'SPICY' project funded by the European Union's Horizon 2020 research and innovation program under grant agreement N°653373. Dr. Serife Kaymaksiz is gratefully acknowledged for providing the PVDF-based graphite electrodes.

References

[1] Q. Zhong, A. Bonakclarpour, M. Zhang, Y. Gao, J.R. Dahn, Synthesis and Electrochemistry of $LiNi_xMn_{2-x}O_4$, J. Electrochem. Soc. 144 (1997) 205–213. doi: 10.1149/1.1837386.

[2] K. Amine, Olivine $LiCoPO_4$ as 4.8 V Electrode Material for Lithium Batteries, Electrochem. Solid-State Lett. 3 (1999) 178-179. doi:10.1149/1.1390994.

[3] E. Peled, The Electrochemical Behavior of Alkali and Alkaline Earth Metals in Nonaqueous Battery Systems—The Solid Electrolyte Interphase Model, J. Electrochem. Soc. 126 (1979) 2047-2051. doi:10.1149/1.2128859.

[4] R. Fong, U. von Sacken, J.R. Dahn, Studies of Lithium Intercalation into Carbons Using Nonaqueous Electrochemical Cells, J. Electrochem. Soc. 137 (1990) 2009–2013. doi: 10.1149/1.2086855.

[5] J. Tarascon, D. Guyomard, New electrolyte compositions stable over the 0 to 5 V voltage range and compatible with the $Li_{1+x}Mn_2O_4$/carbon Li-ion cells, Solid State Ionics. 69 (1994) 293–305. doi:10.1016/0167-2738(94)90418-9.

[6] T. Sato, T. Maruo, S. Marukane, K. Takagi, Ionic liquids containing carbonate solvent as electrolytes for lithium ion cells, J. Power Sources. 138 (2004) 253–261. doi:10.1016/j.jpowsour.2004.06.027.

[7] A.J. Gmitter, I. Plitz, G.G. Amatucci, High Concentration Dinitrile, 3-Alkoxypropionitrile, and Linear Carbonate Electrolytes Enabled by Vinylene and Monofluoroethylene Carbonate Additives, J. Electrochem. Soc. 159 (2012) A370-A379. doi:10.1149/2.016204jes.

[8] G. V. Zhuang, K. Xu, T.R. Jow, P.N. Ross, Study of SEI Layer Formed on Graphite Anodes in PC/LiBOB Electrolyte Using IR Spectroscopy, Electrochem. Solid-State Lett. 7 (2004) A224-A227. doi:10.1149/1.1756855.

[9] Z. Chen, Y. Qin, J. Liu, K. Amine, Lithium Difluoro(oxalato)borate as Additive to Improve the Thermal Stability of Lithiated Graphite, Electrochem. Solid-State Lett. 12 (2009) A69–A72. doi:10.1149/1.3070581.

[10] M. Ishikawa, T. Sugimoto, M. Kikuta, E. Ishiko, M. Kono, Pure ionic liquid electrolytes compatible with a graphitized carbon negative electrode in rechargeable lithium-ion batteries, J. Power Sources. 162 (2006) 658–662. doi:10.1016/j.jpowsour.2006.02.077.

[11] G. Gebresilassie, S. Grugeon, G. Gachot, M. Armand, S. Laruelle, LiFSI vs. $LiPF_6$ electrolytes in contact with lithiated graphite: Comparing thermal stabilities and identification of specific SEI-reinforcing additives, Electrochim. Acta. 102 (2013) 133–141. doi:10.1016/j.electacta.2013.03.171.

[12] V. Etacheri, O. Haik, Y. Go, G.A. Roberts, I.C. Stefan, R. Fasching, D. Aurbach, Effect of Fluoroethylene Carbonate (FEC) on the Performance and Surface Chemistry of Si-Nanowire Li-Ion Battery Anodes, Langmuir. 28 (2012) 965–976. doi: 10.1021/la203712s.

[13] L. Hu, Z. Zhang, K. Amine, Electrochemistry Communications Fluorinated electrolytes for Li-ion battery: An FEC-based electrolyte for high voltage $LiNi_{0.5}Mn_{1.5}O_4$/graphite couple, Electrochem. Commun. 35 (2013) 76–79. doi:10.1016/j.elecom.2013.08.009.

[14] Y. Abu-Lebdeh, I. Davidson, High-Voltage Electrolytes Based on Adiponitrile for Li-Ion Batteries, J. Electrochem. Soc. 156 (2009) A60-A65. doi:10.1149/1.3023084.

[15] X. Sun, C.A. Angell, Doped sulfone electrolytes for high voltage Li-ion cell applications, Electrochem. Commun. 11 (2009) 1418–1421. doi:10.1016/j.elecom.2009.05.020.

[16] S.Y. Lee, K. Ueno, C.A. Angell, Lithium salt solutions in mixed sulfone and sulfone-carbonate solvents: A walden plot analysis of the maximally conductive compositions, J. Phys. Chem. C. 116 (2012) 23915–23920. doi:10.1021/jp3067519.

[17] A. Brenner, Note on an Organic-Electrolyte Cell with a High Voltage, J. Electrochem. Soc. 18 (1971) 461-462. doi:10.1149/1.2408081.

[18] Y. Matsuda, M. Morita, K. Yamada, K. Hirai, Characteristics of Sulfolane-Based Electrolytes for Rechargeable Lithium Batteries, J. Electrochem. Soc. 132 (1985) 2538-2543. doi:10.1149/1.2113619.

[19] S. Tobishima, T. Okada, Lithium cycling efficiency and conductivity for high dielectric solvent/low viscosity solvent mixed systems, Electrochim. Acta. 30 (1985) 1715–1722. doi:10.1016/0013-4686(85)87019-5.

[20] A. Abouimrane, I. Belharouak, K. Amine, Sulfone-based electrolytes for high-voltage Li-ion batteries, Electrochem. Commun. 11 (2009) 1073–1076. doi:10.1016/j.elecom.2009.03.020.

[21] Y. Wang, L. Xing, W. Li, D. Bedrov, Why do sulfone-based electrolytes show stability at high voltages? Insight from density functional theory, J. Phys. Chem. Lett. 4 (2013) 3992–3999. doi:10.1021/jz401726p.

[22] L. Xing, J. Vatamanu, O. Borodin, G.D. Smith, D. Bedrov, Electrode/electrolyte interface in sulfolane-based electrolytes for Li ion batteries: A molecular dynamics simulation study, J. Phys. Chem. C. 116 (2012) 23871–23881. doi:10.1021/jp3054179.

[23] O. Borodin, W. Behl, T.R. Jow, Oxidative stability and initial decomposition reactions of carbonate, sulfone, and alkyl phosphate-based electrolytes, J. Phys. Chem. C. 117 (2013) 8661–8682. doi:10.1021/jp400527c.

[24] A. Lewandowski, B. Kurc, I. Stepniak, A. Swiderska-Mocek, Properties of Li-graphite and $LiFePO_4$ electrodes in $LiPF_6$–sulfolane electrolyte, Electrochim. Acta. 56 (2011) 5972–5978. doi:10.1016/j.electacta.2011.04.105.

[25] S. Li, W. Zhao, X. Cui, Y. Zhao, B. Li, H. Zhang, Y. Li, G. Li, X. Ye, Y. Luo, An improved method for synthesis of lithium difluoro(oxalato)borate and effects of sulfolane on the electrochemical performances of lithium-ion batteries, Electrochim. Acta. 91 (2013) 282–292. doi:10.1016/j.electacta.2013.01.011.

[26] F. Wu, J. Xiang, L. Li, J. Chen, G. Tan, R. Chen, Study of the electrochemical characteristics of sulfonyl isocyanate/sulfone binary electrolytes for use in lithium-ion batteries, J. Power Sources. 202 (2012) 322–331. doi:10.1016/j.jpowsour.2011.11.065.

[27] A. Lewandowski, B. Kurc, A. Swiderska-Mocek, N. Kusa, Graphite/$LiFePO_4$ lithium-ion battery working at the heat engine coolant temperature, J. Power Sources. 266 (2014) 132–137. doi:10.1016/j.jpowsour.2014.04.083.

[28] J. Xia, J. Self, L. Ma, J.R. Dahn, Sulfolane-Based Electrolyte for High Voltage $Li(Ni_{0.42}Mn_{0.42}Co_{0.16})O_2$ (NMC442)/Graphite Pouch Cells, J. Electrochem. Soc. 162 (2015) A1424–A1431. doi:10.1149/2.0121508jes.

[29] J. Xia, J.R. Dahn, Improving sulfolane-based electrolyte for high voltage Li-ion cells with electrolyte additives, J. Power Sources. 324 (2016) 704–711. doi:10.1016/j.jpowsour.2016.06.008.

[30] S. Li, W. Zhao, X. Cui, Y. Zhao, B. Li, H. Zhang, et al., An improved method for synthesis of lithium difluoro(oxalato)borate and effects of sulfolane on the electrochemical performances of lithium-ion batteries, Electrochim. Acta. 91 (2013) 282–292. doi:10.1016/j.electacta.2013.01.011.

[31] S. Solchenbach, M. Metzger, H.A. Gasteiger, Comparative Study of the Anodic and Cathodic

Decomposition of Ethylene Carbonate, Vinylene Carbonate and Fluoroethylene Carbonate, Meet. Abstr. MA2015-02 362 , 228th ECS Meeting, Phoenix, AZ, USA, Oct. 11-15, 2015 http://ma.ecsdl.org/content/MA2015-02/5/362.

[32] M. V. Reddy, G. V. Subba Rao, B.V.R. Chowdari, Metal Oxides and Oxysalts as Anode Materials for Li Ion Batteries, Chem. Rev. 113 (2013) 5364–5457. doi:10.1021/cr3001884.

[33] X. Wu, X. Li, Z. Wang, H. Guo, Y. Peng, Capacity fading reason of $LiNi_{0.5}Mn_{1.5}O_4$ with commercial electrolyte, Ionics. 19 (2013) 379-383. doi: 10.1007/s11581-012-0835-4.

[34] A. Manthiram, K. Chemelewskia and E. Lee, A perspective on the high-voltage $LiMn_{1.5}Ni_{0.5}O_4$ spinel cathode for lithium-ion batteries, Energy Environ. Sci. 7 (2014) 1339-1350. doi: 10.1039/C3EE42981D.

[35] D.Y. Wang, A. Xiao, L. Wells, J.R. Dahn, Effect of Mixtures of Lithium Hexafluorophosphate ($LiPF_6$) and Lithium Bis(fluorosulfonyl)imide (LiFSI) as Salts in $Li[Ni_{1/3}Mn_{1/3}Co_{1/3}]O_2$/Graphite Pouch Cells, J. Electrochem. Soc. 162 (2015) 169–175. doi:10.1149/2.0821501jes.

[36] U.K. Sen, S. Mitra, High-Rate and High-Energy-Density Lithium-Ion Battery Anode Containing 2D MoS_2 Nanowall and Cellulose Binder, ACS Appl. Mater. Interfaces.5 (2013) 1240-1247. doi:10.1021/am3022015.

[37] B. Lestriez, S. Bahri, I. Sandu, L. Roue, D. Guyomard, On the binding mechanism of CMC in Si negative electrodes for Li-ion batteries, Electrochem. Commun. 9 (2007) 2801–2806. doi:10.1016/j.elecom.2007.10.001.

[38] F. Mueller, D. Bresser, E. Paillard, M. Winter, S. Passerini, Influence of the carbonaceous conductive network on the electrochemical performance of $ZnFe_2O_4$ nanoparticles, J. Power Sources. 236 (2013) 87–94. doi: 10.1016/j.jpowsour.2013.02.051.

[39] N.S. Hochgatterer, M.R. Schweiger, S. Koller, P.R. Raimann, T. Wöhrle, C. Wurm, M. Winter, Silicon / Graphite Composite Electrodes for High-Capacity Anodes : Influence of Binder Chemistry on Cycling Stability, Electrochem. Solid-State Lett. 11 (2008) 76–80. doi:10.1149/1.2888173.

[40] D. Bresser, F. Mueller, D. Buchholz, E. Paillard, S. Passerini, Embedding tin nanoparticles in micron-sized disordered carbon for lithium- and sodium-ion anodes, Electrochim. Acta. (2013). doi:10.1016/j.electacta.2013.09.007.

[41] D. Bresser, E. Paillard, R. Kloepsch, S. Krueger, M. Fiedler, R. Schmitz, D. Baither, M. Winter, S. Passerini, Carbon Coated $ZnFe_2O_4$ Nanoparticles for Advanced Lithium-Ion Anodes, Advanced Energy Materials. 128 (2013) 513–523. doi:10.1002/aenm.201200735.

[42] L. El Ouatani, R. Dedryvère, J. Ledeuil, C. Siret, P. Biensan, J. Desbrières, D. Gonbeau, Surface film formation on a carbonaceous electrode: Influence of the binder chemistry, J. Power Sources. 189 (2009) 72–80. doi:10.1016/j.jpowsour.2008.11.031.

[43] H. Buqa, M. Holzapfel, F. Krumeich, C. Veit, P. Novak, Study of styrene butadiene rubber and sodium methyl cellulose as binder for negative electrodes in lithium-ion batteries, J. Power Sources. 161 (2006) 617–622. doi:10.1016/j.jpowsour.2006.03.073.

[44] J.O. Besenhard, J. Yang, M. Winter, Will advanced lithium-alloy anodes have a chance in lithium-ion batteries? J. Power Sources. 68 (1997) 87–90. doi: 10.1016/S0378-7753(96)02547-5.

[45] W. Liu, M. Yang, H. Wu, S.M. Chiao, Enhanced Cycle Life of Si Anode for Li-Ion Batteries by Using Modified Elastomeric Binder, Electrochem. Solid-State Lett. 8 (2005) A100–A103. doi:10.1149/1.1847685.

[46] K. Ui, D. Fujii, Y. Niwata, T. Karouji, Y. Shibata, Y. Kadoma, K. Shimada, N. Kumagai, Analysis of solid electrolyte interface formation reaction and surface deposit of natural graphite negative electrode employing polyacrylic acid as a binder, J. Power Sources. 247 (2014) 981–990. doi: 10.1016/j.jpowsour.2013.08.083.

[47] I. Kovalenko, B. Zdyrko, A. Magasinski, B. Hertzberg, Z. Milicev, R. Burtovyy, I. Luzinov, G. Yushin, A Major Constituent of Brown Algae for Use in High-capacity Li-ion Batteries, Science 334 (2011) 75–80. doi: 10.1126/science.1209150.

[48] S. Komaba, N. Yabuuchi, T. Ozeki, Z. Han, K. Shimomura, H. Yui, Y. Katayama, T. Miura, Comparative Study of Sodium Polyacrylate and Poly-(vinylidene fluoride) as Binders for High Capacity Si Graphite Composite Negative Electrodes in Li-Ion Batteries, J. Phys. Chem. C. 116 (2012) 1380–1389. doi: 10.1021/jp204817h.

Captions

Figure 1. Arrhenius conductivity plot of the 1M $LiPF_6$ SL/DMC 1/1 (wt/wt) electrolyte. (Insert): Voltamperogram at 0.1 mV s^{-1} on Ni (cathodic scan) and Pt (anodic scan) of 1M $LiPF_6$ in SL/DMC 1/1 (wt/wt) and EC/DMC 1/1 (wt/wt). RE and CE: Li.

Figure 2. Discharge capacity and coulombic efficiency of a $LiNi_{0.43}Mn_{1.5}Cr_{0.07}O_4$ electrode in 1M $LiPF_6$ SL/DMC 1/1 (wt/wt) electrolyte. **Insert**: Voltage profiles for the 1^{st}. 2^{nd}, 3^{rd} and 90^{th} cycles. 1C = 147 mA g^{-1}

Figure 3. (a) Comparison of discharge capacity and efficiency between a PVDF-based (3.2 mg cm^{-2} AM mass loading) and a CMC/SBR-based electrode (5.4 mg cm^{-2} AM mass loading). **(b)** Comparison of the voltage profiles for selected cycles. Cycle numbers are indicated next to the curves. 1C = 372 mA g^{-1}.

Figure 4. (a) Capacity retention and cycling efficiency of a Graphite/NMC Li-ion cell (3 electrodes cell, reference Li metal). AM mass loading cathode: 14.5 mg cm^{-2}, AM mass loading anode: 6 mg cm^{-2}. Voltage range: 2.8V-4.5 V. rates indicated on the figure. **(b)** Corresponding potential profile for the NMC cathode and the graphite anode. Cycle numbers are indicated on the curves.

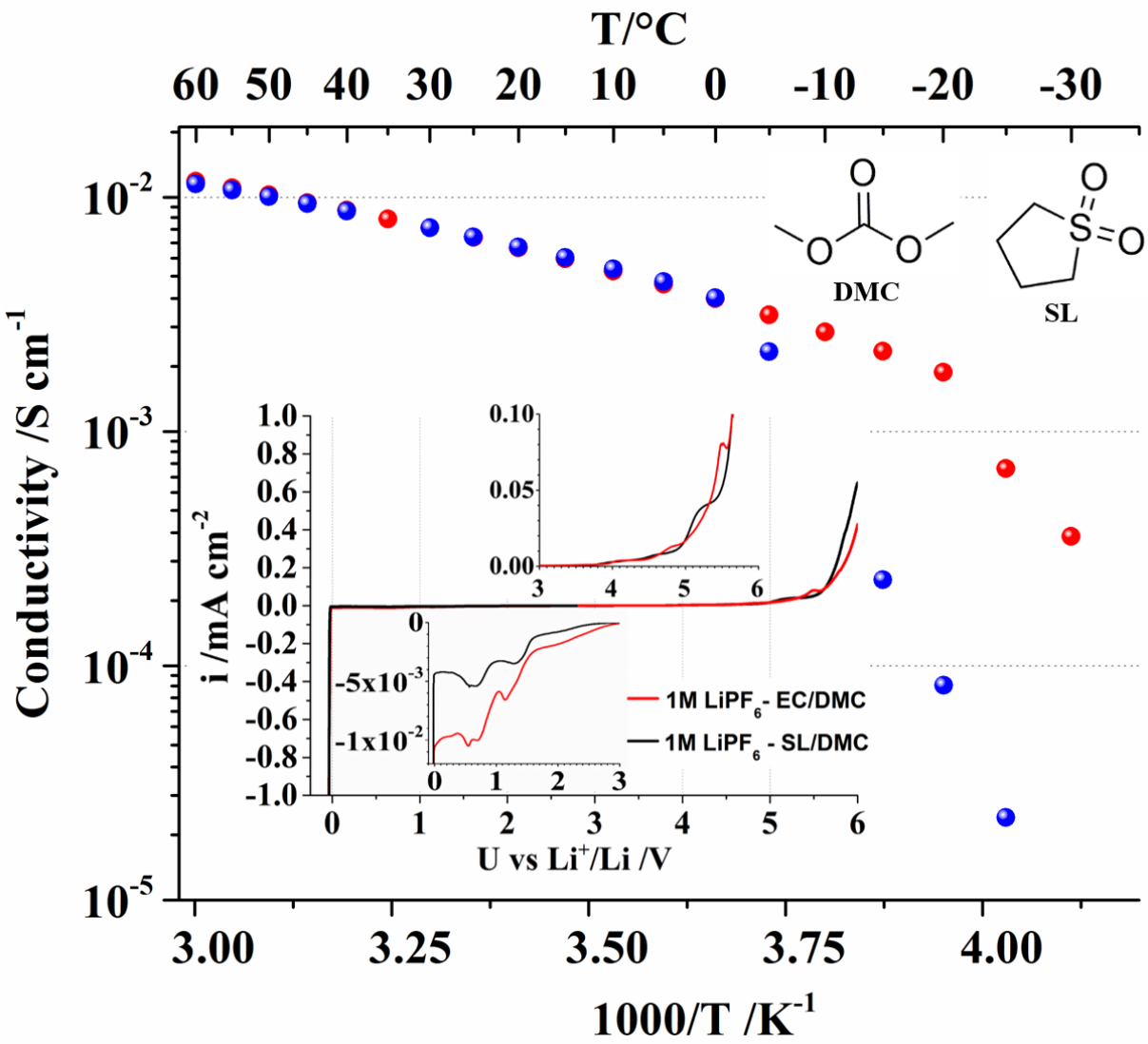
T/°C
60 50 40 30 20 10 0 -10 -20 -30
Conductivity /S cm-1
10-2
10-3
10-4
10-5
3.00 3.25 3.50 3.75 4.00
1000/T /K-1
DMC
SL
i /mA cm-2
U vs Li+/Li /V
1M LiPF6 - EC/DMC
1M LiPF6 - SL/DMC

Figure 1

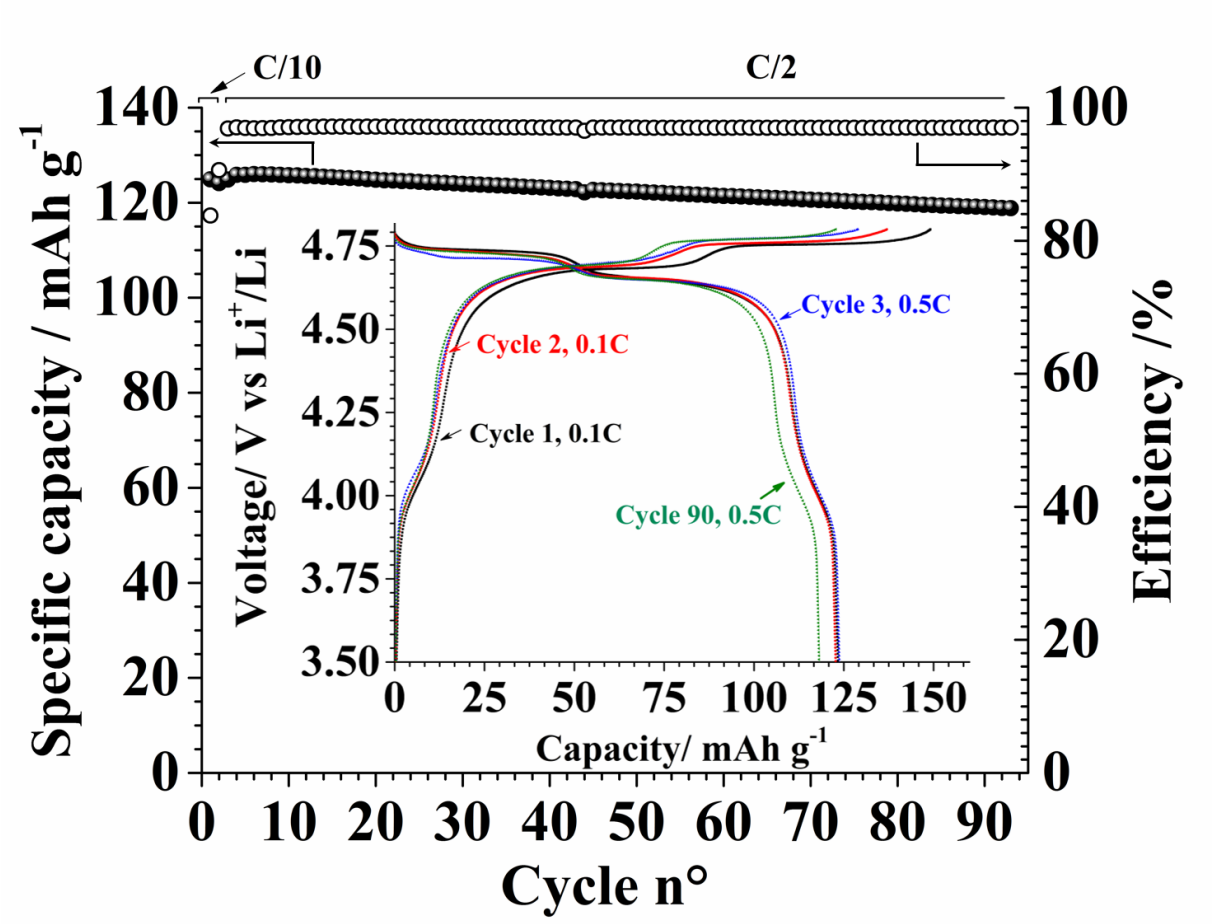
C/10
C/2
Specific capacity / mAh g-1
Efficiency /%
Cycle n°
Voltage/ V vs Li+/Li
Capacity/ mAh g-1
Cycle 1, 0.1C
Cycle 2, 0.1C
Cycle 3, 0.5C
Cycle 90, 0.5C

Figure 2

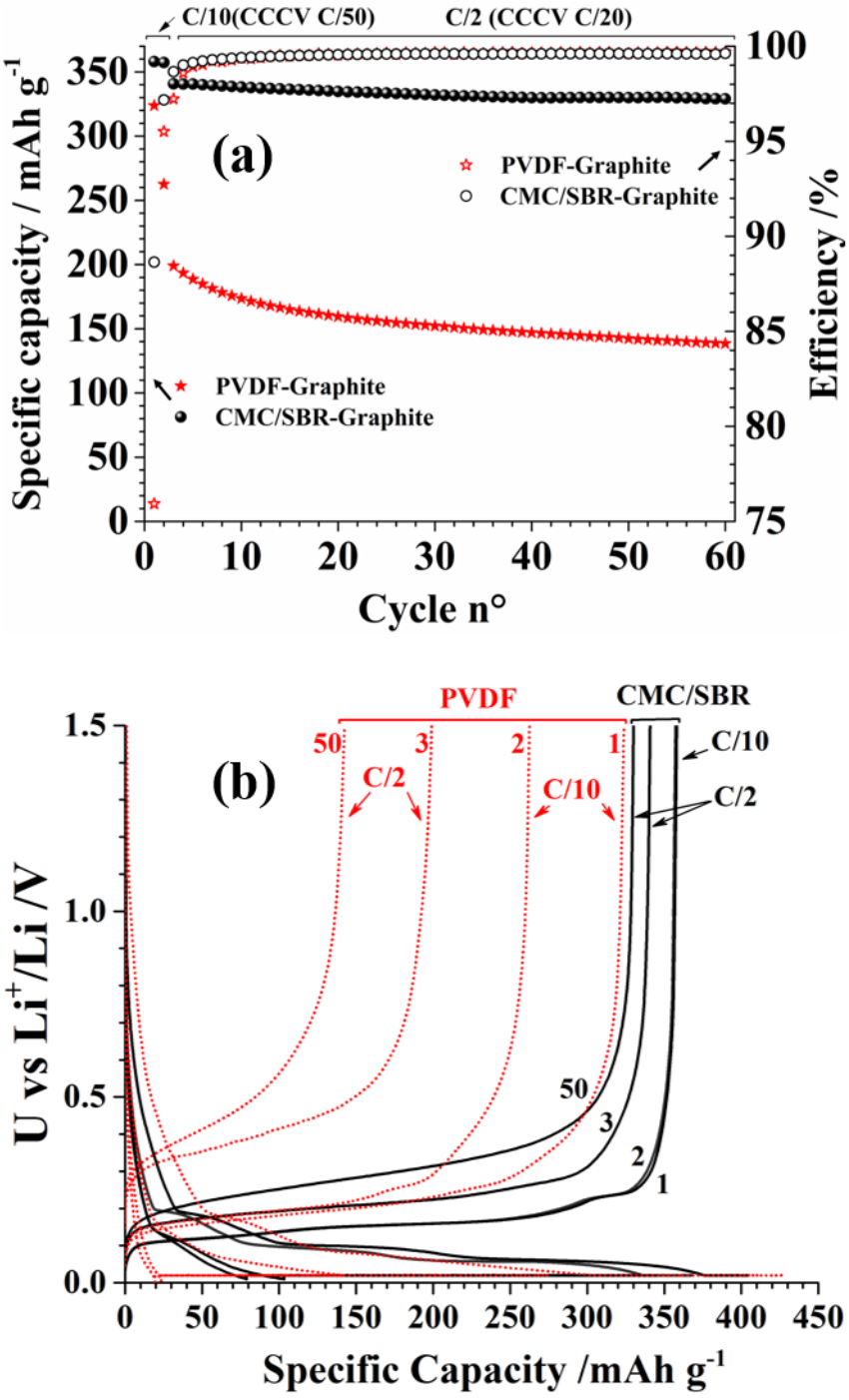
C/10(CCCV C/50)
C/2 (CCCV C/20)
(a)
PVDF-Graphite
CMC/SBR-Graphite
PVDF-Graphite
CMC/SBR-Graphite
Specific capacity / mAh g-1
Efficiency /%
Cycle n°
(b)
PVDF
CMC/SBR
C/2
C/10
C/10
C/2
50
3
2
1
U vs Li+/Li /V
Specific Capacity /mAh g-1

Figure 3.

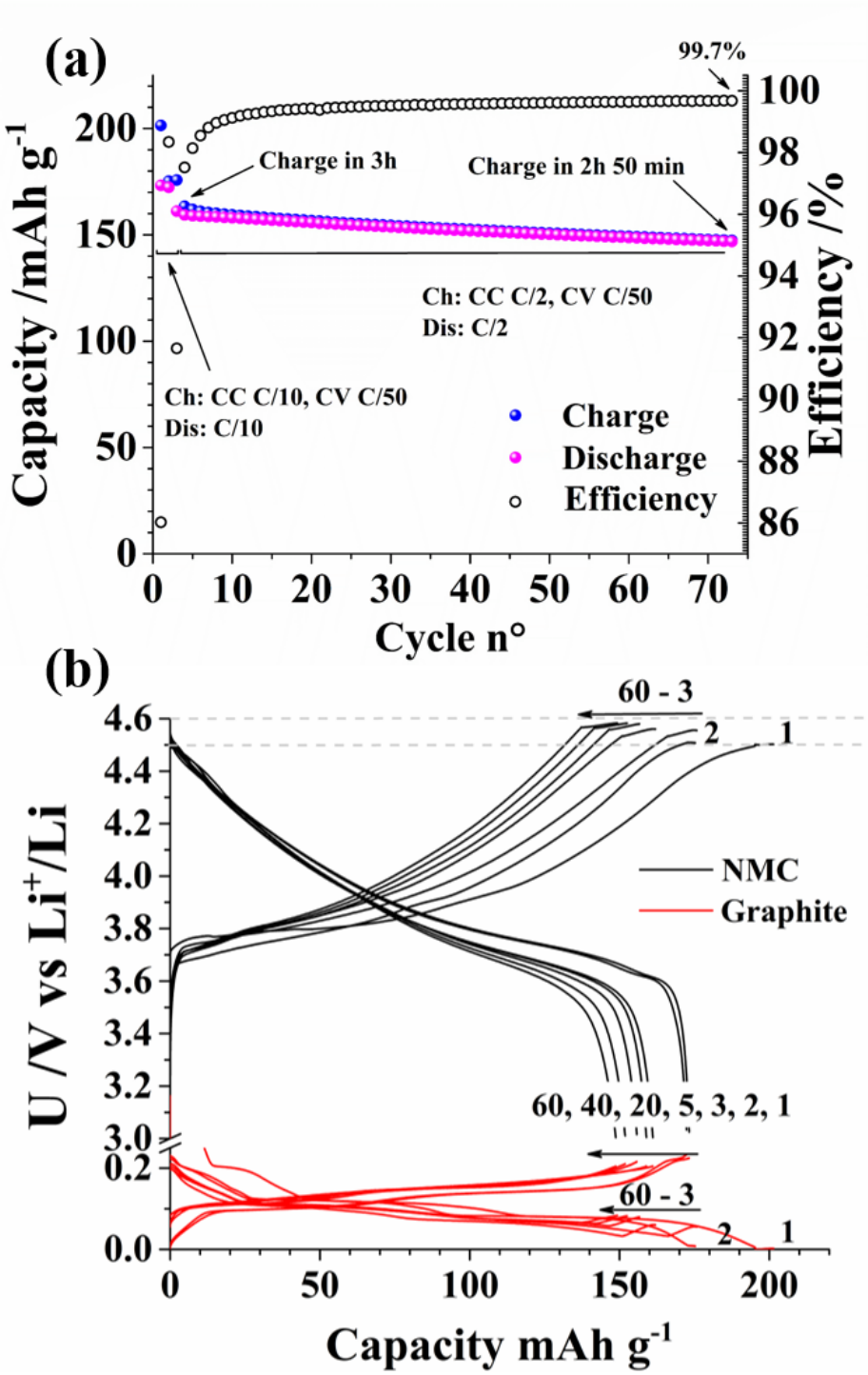
(a)
99.7%
Capacity /mAh g-1
Efficiency /%
Charge in 3h
Charge in 2h 50 min
Ch: CC C/2, CV C/50
Dis: C/2
Ch: CC C/10, CV C/50
Dis: C/10
Charge
Discharge
Efficiency
Cycle n°
(b)
60 - 3
2
1
NMC
Graphite
U /V vs Li+/Li
60, 40, 20, 5, 3, 2, 1
Capacity mAh g-1

Figure 4.